Low-Temperature Reduction of NO_2 on Oxidized Mo(110)

L. J. Deiner, D.-H. Kang, and C. M. Friend*

Department of Chemistry and Division of Engineering and Applied Science, Harvard University, 12 Oxford Street, Cambridge, Massachusetts 02138

Received: August 19, 2004; In Final Form: March 25, 2005

The reactions of nitrogen dioxide (NO_2) were investigated on oxidized Mo(110) containing both chemisorbed oxygen and a thin film oxide. NO_2 reacts on both oxidized Mo(110) surfaces via a combination of reversible adsorption and reduction to NO, N_2, and trace amounts of N_2O below 200 K. On the surface containing chemisorbed O, there is some complete dissociation of NO_2 to yield N(a) and O(a). N_2 forms at high temperatures through atom combination. On both surfaces, NO is the predominant product of NO_2 reduction. However, the chemisorbed layer which has a low oxidation state, and hence a greater capacity to accept oxygen, more effectively reduces NO_2. The selectivity for N_2 formation over N_2O is greater for NO_2 as compared with NO on both surfaces studied. The selectivity changes are largely attributed to an increase in the concentration of Mo═O species and a change in the distribution of oxygen on the surface. Notably, more oxygen, in particular Mo═O moieties, is deposited by NO_2 reaction than by O_2 reaction, indicating that NO_2 is a stronger oxidant. The fact that there are several N-containing species on the surface at low temperatures may also affect the product distribution. On both surfaces, N_2O_4, NO_2, and NO are identified by infrared spectroscopy upon adsorption at 100 K. All N_2O_4 desorbs by 200 K, leaving only NO_2 and NO on the surface. Infrared spectroscopy of NO_2 on ^{18}O-labeled surfaces provides evidence for oxygen transfer or exchange between different types of sites even at low temperatures.

Introduction

Nitrogen oxides (NO, NO_2, and N_2O) are produced during combustion processes due to N-containing impurities in fuels and due to thermal reaction of nitrogen and oxygen in the air. Because nitrogen oxides lead to smog and acid rain, much current research is devoted to devising effective methods of NO_x emission reduction from stationary and automotive sources. Various studies of this Pt-based technology have suggested that NO, the most common form of NO_x produced by cars, is much more efficiently reduced after an initial oxidation step to NO_2.[1,2] Nitrogen dioxide is also thought to be important in plasma-assisted NO_x reduction.[2] The intense interest in these processes has stimulated a large number of studies of NO and NO_2 on single-crystal metal surfaces as model systems.

Heterogeneous NO_x reactions are also important from the perspective of atmospheric chemistry.[3,4] Through various complex and intertwined reaction cycles, it is believed that NO_2 plays a role in determining atmospheric concentrations of HNO_3 and O_3.[4] Some atmospheric NO_2 reactions occur on ice particles or on soot, while others occur on metal oxide surfaces, such as dust particles.[4] While the conditions differ markedly for these important processes involving the heterogeneous chemistry of NO_2 and those employed in model systems, insights into the heterogeneous reactions of NO_x are gained from studies of single-crystal studies.

Previous studies show that the heterogeneous reactions of NO_2 depend on the strength of oxygen binding to the various surfaces studied. For Au(111), the adsorption of NO_2 is completely reversible.[5] However, partial dissociation is the predominant pathway for Ag(111),[6] Ag(110),[7] Pt(111),[8] Pd(111),[9] Ru(001),[10] and clean and Pd-covered Rh(111).[11] In some cases, the partial decomposition is self-limiting, leading to molecular NO_2 chemisorption or nitrate formation at high coverages. The reaction pattern of initial dissociation leading to partial surface passivation followed by molecular adsorption has also been found for W(110), a highly active refractory metal.[12] For NO_2 dosed onto Mo(110) at 100 K, any molecularly adsorbed NO_2 dissociates into NO(a), N(a), and O(a) by 150 K.[13]

The reactivity of NO_2 on metal oxides also varies widely, ranging from complete decomposition to nitrate formation. For adsorption of NO_2 on CeO_2,[14] MgO,[15] TiO_2,[16] Fe_2O_3,[17] and ZnO,[18] the formation of adsorbed nitrate is the main pathway; small amounts of NO_2 remain molecularly adsorbed, but there is no full decomposition.[19] It has been shown, both experimentally and theoretically, that it is also possible to manipulate the composition and vacancy density of oxides to open up N−O bond scission pathways. For example, mixed metal oxides of Cr and Mg, Cr_2O_3, and partially reduced CeO_2 are oxides that readily induce the loss of oxygen from NO_2 to yield NO even at low temperatures.[15,20,21] As such, dopants and vacancies have been credited with inducing structural and electronic changes which favor N−O bond scission.[15,19] However, the role of vacancies and dopants is not entirely general: on partially reduced Ce/Zr mixed metal oxides, reversible molecular adsorption of NO_2 predominates.[19]

In the present work, we investigate the effect of oxygen coordination and the extent of surface oxidation on the reactions of NO_2 on oxidized Mo(110). We use infrared spectroscopy to identify a complex mixture of N-containing species, including N_2O_4, NO_2, NO, and dinitrosyl. A combination of reversible adsorption and decomposition to NO(a) and O(a) is observed, which indicates that surface oxygen stabilizes the NO_2 on Mo but does not entirely eliminate the tendency toward oxygen

* Corresponding author. Fax: 617 496 8410. Phone: 617 495 4052. E-mail: friend@chemistry.harvard.edu.

10.1021/jp046249a CCC: $30.25
Published on Web 06/10/2005

abstraction. In addition, there is a small amount of complete dissociation on the O-covered surface. The O-covered surface has a slightly higher overall reactivity than the thin film oxide, and the selectivity for reduction products is also slightly higher.

Experimental Section

All experiments were performed in a stainless steel ultrahigh vacuum chamber described in detail elsewhere.[22] The chamber has a base pressure of $\sim 1 \times 10^{-10}$ Torr and is equipped with a quadrupole mass spectrometer (UTI model 100C), an Auger electron spectrometer, and low-energy electron diffraction (LEED) optics. The vacuum chamber is interfaced with a Fourier transform infrared spectrometer (Thermo Nicolet Nexus 670).

The oxygen overlayer was prepared by directed dosing of O_2 at 100 K followed by transient heating to 500 K ($dT/dt \sim$ 10 K/s). This procedure saturates high coordination sites without inducing oxygen dissolution into the bulk.[23] The saturated oxygen overlayer on Mo(110) shows a (1×6) low-energy electron diffraction pattern (not shown). As terminal oxygen forms from the decomposition of adsorbed NO_2 at high temperatures, the low-energy electron diffraction pattern changes to a diffuse (1×1) pattern, indicating that additional oxygen from NO_2 initiates the rearrangement of surface oxygen, inducing crowding or disorder in the layer.

The thin film oxide was prepared by dosing O_2 at 1200 K followed by rapid annealing to 1400 K ($dT/dt \sim 20$ K/s). The resulting surface consists of subsurface oxygen and oxygen in high coordination sites. No terminal oxygen is present.[23] A complex LEED pattern with sharp spots is obtained for the thin film oxide.[24]

NO_2 (Specialty Gases) was used as received without further purification. Gas was introduced through a stainless steel manifold and doser. Saturation coverage, defined as the coverage immediately preceding multilayer sublimation, was achieved by directed dosing corresponding to a background pressure rise of $\sim 3 \times 10^{-10}$ Torr for 75 s. The doser was conditioned so as to minimize NO_2 dissociation by heating all stainless steel surfaces to 373 K in the presence of NO_2 for 2.5 h. In addition, the manifold was outfitted with gold-plated copper gaskets to prevent corrosion. The purity of the NO_2 dosed through the baked manifold was confirmed by mass spectrometry of condensed multilayers. A trap containing MgO was installed inline before the turbomolecular pumping system in order to prevent degradation of the pump. Safety of personnel was assured by a handheld NO_x detector (Bacharach, Nonoxor II). Dosing was performed while the crystal was biased at -90 V to prevent electron induced reactions from stray electrons originating at the ion gauge.[25]

Temperature programmed reaction was performed while the crystal was biased at -90 V in order to prevent reactions induced by the mass spectrometer filament. Radiative heating (average $dT/dt \sim 10$ K/s) was used to reach temperatures up to 800 K. Electron bombardment heating was used to reach temperatures above 800 K (average $dT/dt \sim 15$ K/s). The filament used to heat the crystal was briefly flashed to operational currents prior to each data collection run. This prevented artifacts of filament outgassing in the data. Some CO was detected during temperature programmed reaction experiments, perhaps from displacement of CO from the mass spectrometer shield. The m/z 28 trace was corrected for the CO by measuring the m/z 12 signal and correcting the data for this spurious signal. We confirmed that the residual 28 amu signal below 200 K is due to N_2 based on the fact that $^{14}N^{15}N$ is formed during programmed reaction experiments performed following the adsorption of ^{15}NO followed by dosing with NO_2 on the chemisorbed oxygen overlayer. No correction of the 28 trace was made for N_2O fragmentation, since the yield of N_2O is small and the m/z 28:44 ratio is 1:10 for N_2O.

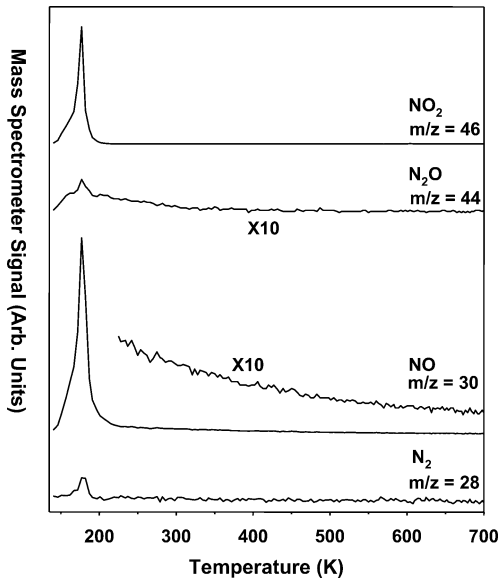

Figure 1. Temperature programmed reaction data following the exposure of NO_2 to a thin film oxide of Mo(110) at a dose sufficient to produce multilayers of NO_2 ($\Delta p(NO_2) = 3 \times 10^{-10}$ Torr, $\Delta t = 75$ s). The NO_2 was dosed using a directed doser. Data are uncorrected for fragmentation.

Infrared spectra were collected with the crystal temperature at $\sim$120 K. Five hundred scans were recorded per experiment. The resolution was set to 4 cm^{-1}, and data were collected using a liquid nitrogen cooled MCT-A semiconductor photodiode detector. Background spectra were obtained after heating the sample to 760 K for the chemisorbed layer and 1200 K for the thin film oxide.

Results

Temperature Programmed Reaction on the Thin Film Oxide. A combination of reversible molecular adsorption, partial decomposition to NO(a) and O(a), and reduction to N_2 and trace amounts of N_2O is observed for NO_2 reaction on the thin film oxide (Figure 1). NO_2 desorbs in a peak at $\sim$170 K, which is similar to the temperature 175 K reported for the desorption of NO_2 from O-covered Pt(111).[26] There is no evolution of either O atoms or O_2 during temperature programmed reaction. Oxygen remains bound to the Mo up to 2000 K, at which point volatile Mo_xO_y species are produced.

The predominant product in temperature programmed reaction is gaseous NO, accounting for over 50% of the total reaction products (Table 1). NO is evolved in two peaks: a sharp feature at 170 K and a broad tail in the range 100−600 K for all coverages studied. The high-temperature NO tail was observed previously in the temperature programmed reaction of NO on a thin film oxide of Mo(110).[27] While there is a significant contribution to the 170 K peak in the 30 amu data due to fragmentation of NO_2, it does not account entirely for the peak (Figure 1). Specifically, the m/z 30:m/z 46 ratio for NO_2 multilayers is 2.3:1 This ratio is 3.5:1 for the 170 K peak.

N−N coupling products are also produced below 200 K during reaction of NO_2 on the thin film oxide: N_2 and a trace amount of N_2O. Dinitrogen accounts for $\sim$13% of the reaction products below 600 K. No N_2O formation is detected in temperature programmed reaction data obtained for low expo-

TABLE 1: Relative Yields of Products from NO_2 Reaction on a Thin Film Oxide Formed on Mo(110) as Compared to Relative Yields of Products from NO Reaction on the Same Surfaces[a] (Yields Are Expressed as a Function of Total Reaction on Each Surface, and Traces Are Corrected for Fragmentation from Higher Masses but Not for Ionization Efficiency Differences)

Θ_O	N_2	NO	N_2O	NO_2	N_2 (recomb.)
NO_2, saturation coverage	0.13	0.57	<0.04	0.27	0.00
NO_2, low coverage	0.16	0.56	<0.05	0.22	0.00
NO[b]	0.25	0.46	0.29	0.00	0.00

[a] From Queeney et al.[23] [b] Terminal oxygen sites already populated prior to NO dosing.

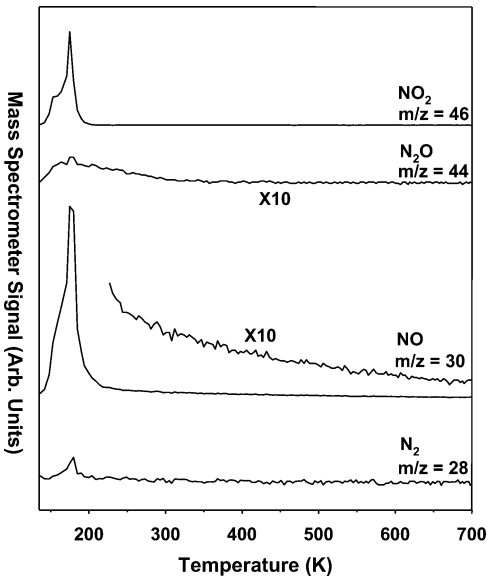

Figure 2. Temperature programmed reaction data for NO_2 on Mo(110)−(1 × 6)−O at at a dose sufficient to produce multilayers of NO_2 ($\Delta p(NO_2) = 2 \times 10^{-10}$ Torr, $\Delta t = 90$ s). The NO_2 was dosed using a directed doser. Data are uncorrected for fragmentation.

sures of NO_2, and only trace amounts ($\leq$4%) are formed even at high coverages. No N-containing products are detected above 600 K. Specifically, no N_2 is detected between 600 and 1600 K (data not shown).

The selectivity for reaction on the thin film oxide depends on the amount of NO_2 dosed on the surface such that there is a greater degree of oxygen loss at low NO_2 coverages (Table 1). While the majority of product is still NO for low NO_2 coverages, accounting for 56% of the gaseous products, the yields of N−N coupling products, N_2 and N_2O, increase slightly to 16 and ~5%, respectively. The fraction of the NO_2 that reversibly adsorbs is 22%, as compared to 27% for NO_2 at saturation coverage.

Temperature Programmed Reaction on Mo(110)−(1 × 6)−O. The products of NO_2 reaction on O-covered Mo(110) are the same as those observed on the thin film oxide—NO_2, NO, N_2O, and N_2—albeit with some differences in quantity (Figure 2). In contrast to the thin film oxide, there is some complete dissociation of NO_2 to N(a) and O(a) on Mo(110)−(1 × 6)−O that ultimately leads to N_2 formation at 1400 K via atom combination (data not shown). In addition, there is more N_2 formation overall and a stronger dependence on NO_2 coverage in the selectivities in comparison to the thin film oxide. As for the thin film oxide, there is no detectable production of either O atoms or O_2 during temperature programmed reaction.

There is a greater propensity for complete oxygen loss from NO_2 at low coverages for reaction on Mo(110)−(1 × 6)−O (Table 2). The selectivity for NO formation is ~64% at saturation coverage and ~32% at low NO_2 coverages (Table 2). The decrease in NO yield at low NO_2 coverages is accompanied by an increase in the yield of N_2 below 200 K: ~28% at low NO_2 coverages versus ~15% at saturation coverage. The relative yield of N_2O also depends on the initial NO_2 exposure: N_2O production accounts for <2% of the products at saturation coverage but 9% at low NO_2 coverages. Finally, the yield of N_2 at high temperatures, due to atom combination, is ~3% at saturation coverage and ~17% at low coverages (Table 2), indicating that deposition of oxygen at low temperatures via NO_2 reaction inhibits complete dissociation.

TABLE 2: Relative Yields of Products from NO_2 Reaction on Mo(110)−(1 × 6)−O as Compared to Relative Yields of Products from NO Reaction on the Same Surfaces[a] (Yields Are Expressed as a Function of Total Reaction on Each Surface, and Traces Are Corrected for Fragmentation from Higher Masses but Not for Ionization Efficiency Differences)

Θ_O	N_2	NO	N_2O	NO_2	N_2 (recomb.)
NO_2, saturation coverage	0.15	0.64	<0.02	0.16	0.03
NO_2, low coverage	0.28	0.32	<0.09	0.15	0.17
NO[a]	0.28	0.23	0.35	0.00	0.14

[a] From Queeney et al.[23]

Infrared Reflectance Absorbance Spectroscopy on Mo(110)−(1 × 6)−O. Infrared spectroscopy provides evidence for condensed N_2O_4, Mo-bound N_2O_4, NO (both monomeric and dinitrosyl species), and terminal oxygen upon exposure of NO_2 at 110 K (Figure 3a, Table 3). Peaks characteristic of condensed N_2O_4 are the $\delta_s(NO_2)$ mode at 784 cm^{-1}, the $\nu_s(NO_2)$ mode at 1296 cm^{-1}, and the $\nu_{as}(NO_2)$ mode at 1763 cm^{-1}. These assignments are made on the basis of agreement with previous studies of N_2O_4 on Ru and gold foil and N_2O_4 in inert matrixes.[10,28,29] The peaks at 1260 and 1910 cm^{-1} are assigned respectively as the $\nu_s(NO_2)$ and $\nu_{as}(NO_2)$ modes of monolayer N_2O_4. These features are similar in energy to D′ N_2O_4 identified in inert matrixes.[28] Other possible assignments of the peak at 1910 cm^{-1} are weakly bound NO[30] or the ν(NO) mode of N_2O_3 on Au(111).[31] Both of these assignments are ruled out on the basis of the fact that there is no measurable increase in the intensity of the 1910 cm^{-1} peak when $^{14}N^{16}O$ is dosed after NO_2 on Mo(110)−(1 × 6)−O (data not shown). This provides strong evidence that the 1910 cm^{-1} peak is not the ν(NO) mode of N_2O_3 formed from adsorbed NO_2 and impinging gas phase NO.

In addition to N_2O_4, two types of molecular NO are identified on the surface: monomeric NO and a dinitrosyl species (entailing bonding of two NO molecules to one metal). The dinitrosyl peak is at 1826 cm^{-1}, the same frequency as that observed for dinitrosyl made from NO on O-modified Mo(110).[32] The monomeric NO peak at 1740 cm^{-1} is similarly identified on the basis of comparison to previous work with NO on O-modified Mo(110).

Infrared spectroscopy also provides evidence for the dissociation of NO_2 at low temperatures that leads to the deposition of terminal oxygen at low temperatures. Terminal oxygen is signified by the presence of the ν(Mo═O) peak at 980 cm^{-1} at 110 K (Figure 3).[33] The assignment is confirmed by the development of two peaks at 980 and 950 cm^{-1} when NO_2 reacts on Mo(110)−(1 × 6)−^{18}O. These data further show that NO_2 is capable of displacing oxygen bound in high coordination sites to terminal sites even at low temperatures.

The assignments of the peaks at 784, 1296, and 1763 cm^{-1} to multilayer N_2O_4 are confirmed by the fact that they disappear upon heating to 160 K (Figure 3b, Table 4). The peaks visible

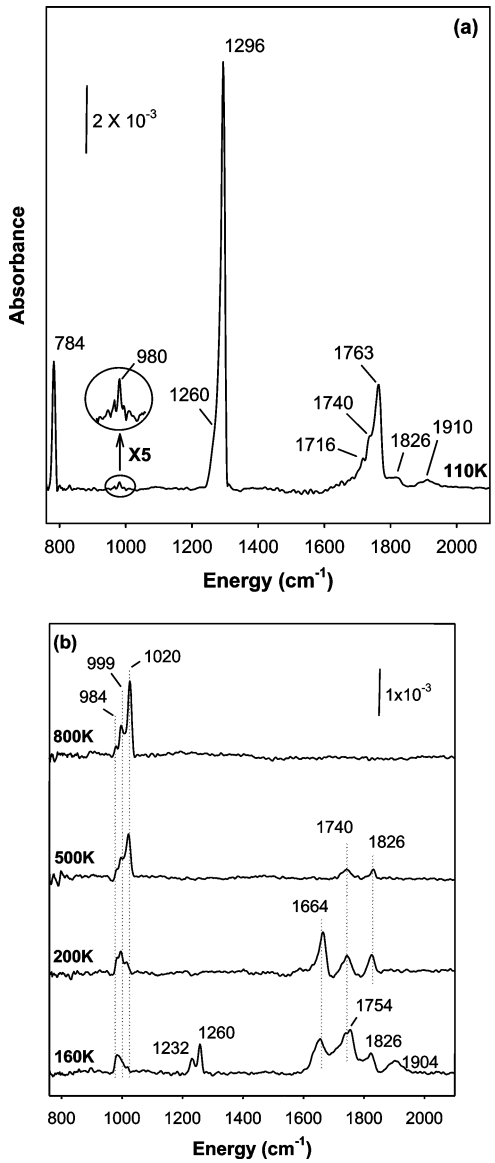

Figure 3. Infrared spectra obtained after condensation of NO_2 multilayers on Mo(110)−(1 × 6)−O at 110 K: (a) as prepared; (b) after heating to temperatures in the range 160−800 K.

TABLE 3: Assignments for Vibrational Bands of Various NO_x Species Formed from NO_2 on O-Modified Mo(110) upon Adsorption at 110 K

frequency (cm^{-1})	assignment
784	$\delta(NO_2)$ of N_2O_4 multilayer
980	ν(Mo═O)
1260	$\nu_s(NO_2)$ of N_2O_4 monolayer
1296	$\nu_s(NO_2)$ of N_2O_4 multilayer
1716	$\nu_{as}(NO_2)$ of N_2O_4 multilayer
1740	ν(NO) of monomeric NO
1763	$\nu_{as}(NO_2)$ of N_2O_4 multilayer
1826	ν_s(NO) of dinitrosyl
1910	$\nu_{as}(NO_2)$ of N_2O_4 monolayer

after heating to 160 K are at 990 (with a shoulder at ∼1000 cm^{-1}), 1232, 1260, 1664, 1754, 1826, and 1904 cm^{-1} (Figure 3b). This indicates that the species present after heating to 160 K are monolayer N_2O_4, NO_2, NO, dinitrosyl, and terminal oxygen (Figure 3b, Table 4).

The peak at 1664 cm^{-1} is attributed to the $\nu_{as}(NO_2)$ mode of monomeric NO_2 on the basis of agreement with literature values for matrix-isolated NO_2.[34] The possibility that this peak is due to monomeric NO was considered but ruled out on the basis of

TABLE 4: Assignments of Peaks for Infrared Spectra Obtained after Heating NO_2 on Mo(110)−(1 × 6)−O to Various Temperatures

assignment	160 K	200 K	500 K	800 K
ν(Mo═O)	984	984	984	984
	996	996	996	996
	1020	1020	1020	1020
$\nu_s(NO_2)$ of N_2O_4 monolayer	1232			
$\nu_s(NO_2)$ of N_2O_4 monolayer	1260			
$\nu_{as}(NO_2)$ of NO_2	1664	1664		
ν(NO) of monomeric NO	1740	1740	1740	
ν(NO) of monomeric NO	1754			
ν_s(NO) of dinitrosyl	1826	1826	1826	
$\nu_a(NO_2)$ of N_2O_4 monolayer	1904			

the fact that the peak does not shift when ^{15}NO is dosed on the NO_2-containing surface annealed to 170 K (data not shown). Similarly, the possibility that the 1664 cm^{-1} peak corresponds to NO_3 was discounted on the basis of analogy with isotopic labeling experiments on the thin film oxide (see below).

The peaks at 1232, 1260, and 1904 cm^{-1} are assigned to monolayer N_2O_4 adsorbed to the surface (Table 4). The intensities of the peaks attributed to monolayer N_2O_4 at 1230 and 1260 cm^{-1} decrease as a function of temperature, ultimately disappearing after heating to 200 K (Figure 3b). The disappearance of the peaks assigned to N_2O_4 correlates with the desorption of NO_2 in temperature programmed reaction experiments. The only peaks remaining on the surface after heating to 200 K are NO_2, NO, dinitrosyl, and terminal oxygen on the surface.

The assignments made to the dinitrosyl and monomeric NO, 1826 and 1740 cm^{-1}, respectively, are confirmed by experiments in which ^{15}NO is exposed to the surface after first adsorbing NO_2 and subsequently heating to 300 K (Figure 4, Table 5). New peaks appear at 1699 and 1784 cm^{-1} after dosing ^{15}NO. The peak at 1699 cm^{-1} is assigned to monomeric ^{15}NO downshifted from 1740 cm^{-1}, whereas the peak at 1784 cm^{-1} is assigned to the $\nu_s(^{15}NO)$ mode of $(^{15}NO)_2$ downshifted from 1826 cm^{-1}. The peaks for both $(^{15}NO)_2$ and $(^{14}NO)_2$ are the same as those previously reported for dinitrosyl species formed from NO on this surface.[35] Interestingly, there is no observable intensity in the region expected for the mixed-isotope dinitrosyl

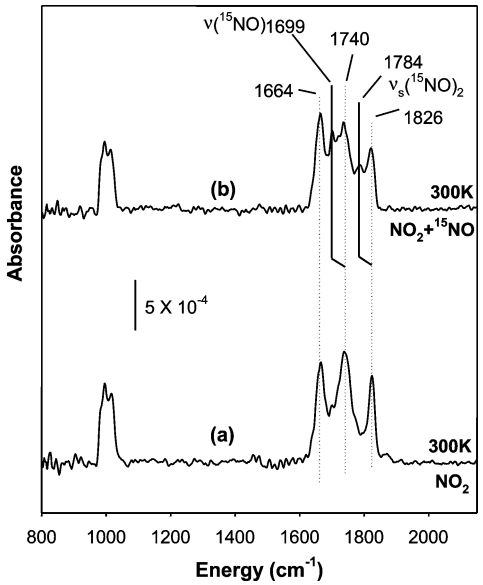

Figure 4. Infrared spectra of (a) NO_2 on Mo(110)−(1 × 6)−O annealed to 300 K and (b) ^{15}NO dosed on NO_2 on Mo(110)−(1 × 6)−O annealed to 300 K.

TABLE 5: Assignments of Peaks for Infrared Spectra Obtained after Exposing ^{15}NO to Mo(110)−(1 × 6)−O Followed by NO_2 Adsorption and Subsequently Heating to 300 K

	frequency (cm^{-1})	
assignment	pure NO_2	$^{15}NO + NO_2$
$\nu_{as}(NO_2)$ of NO_2	1664	1664
$\nu(^{15}NO)$ of monomeric NO		1699
$\nu(NO)$ of monomeric NO	1740	1740
$\nu_s(^{15}NO)$ of dinitrosyl		1784
$\nu_s(NO)$ of dinitrosyl	1826	1826

($^{15}NO^{14}NO$), indicating that the dinitrosyl, once formed, is a stable species

Upon annealing to 500 K, the NO_2 (1664 cm^{-1}) feature disappears, leaving only the monomeric and dinitrosyl NO (1740 and 1826 cm^{-1}) and the terminal oxygen species (Figure 3, Table 4). Simultaneously, the intensity in the terminal oxygen region redistributes, indicating an increase in the population of terminal oxygen adjacent to vacancies.[33] Further heating to 800 K induces the disappearance of all residual surface NO_x species and leads to an increase in the resolution of the terminal oxygen region (Figure 3).

Infrared Reflectance Absorbance Spectroscopy on the Thin Film Oxide. The infrared spectrum of NO_2 on the Mo(110)−(1 × 6)−O surface is qualitatively similar to the infrared spectrum of NO_2 on the thin film oxide (Figure 5). Further, the temperature evolution of the spectra is essentially the same. As mentioned above, the possibility that the 1664 cm^{-1} peak is due to NO_3 was ruled out on the basis of the fact that the peak position does not shift when NO_2 is adsorbed on an ^{18}O-labeled thin film oxide (data not shown). Since NO_2 is capable of displacing oxygen from high coordination sites at low temperatures, ^{18}O would be incorporated into a surface nitrate.

The most notable difference between the spectra of NO_2 on the Mo(110)−(1 × 6)−O and thin film oxide surfaces is the distribution of intensity in the terminal oxygen region. On the Mo(110)−(1 × 6)−O surface, the 1020 cm^{-1} peak is the most intense terminal oxygen stretch, whereas the intensities of the 980, 996, and 1020 cm^{-1} peaks are approximately the same on the thin film oxide. These data indicate a more equal distribution of terminal oxygen among step sites, terrace sites, and sites adjacent to vacancies.

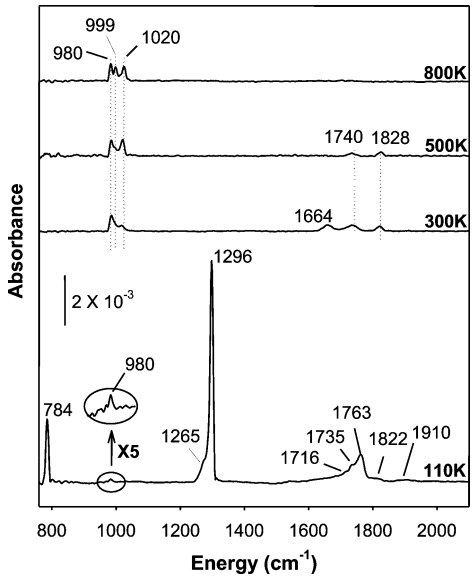

Figure 5. Infrared spectra of the region from 750 to 2100 cm^{-1} for multilayers of NO_2 condensed on a thin film oxide of Mo(110) as dosed at 110 K and then annealed to 300, 500, and 800 K.

Discussion

NO_2 readily loses oxygen to O-modified Mo(110), which is generally consistent with the strong Mo−O bond energy and the low oxidation state of the surface. The loss of oxygen to the surface is signified by the deposition of terminal oxygen from NO_2 reaction on both the thin film and the chemisorbed oxygen layer. Interestingly, NO_2 is a stronger oxidant of Mo(110) than O_2, based on the fact that higher coverages of oxygen can be achieved using NO_2. Furthermore, isotopic labeling experiments demonstrate that oxygen, although strongly bound to Mo, is displaced at 110 K by oxygen from the NO_2 reaction, suggesting that it is mobile, that is, that it can move from one site to another, on the surface. Indeed, oxygen has been shown to be mobile on TiO_2 using STM,[36] indicating that strongly bound oxygen is mobile on many surfaces.

The selectivity for NO_2 reduction is linked to the amount of oxygen on the surface. In the limiting case of initially clean Mo(110), all NO_2 dissociates by 150 K.[13] Our results are generally consistent with those reported for the clean Mo(110) surface that indicated that NO is the primary product of NO_2 reaction. At low NO_2 doses on Mo(110)−(1 × 6)−O, the ratio of low-temperature N_2:NO is similar for NO and NO_2 reaction (Table 2). At low NO_2 exposures, there is a relatively small amount of Mo═O deposited, and therefore, the state of the surface more closely resembles that for NO reaction on the freshly prepared Mo(110)−(1 × 6)−O. The relative amount of NO evolved from NO itself is lower than that from NO_2, which is consistent with some dissociation of NO on a surface with lower oxygen coverage. Some complete dissociation to adsorbed N and O is observed for both NO and NO_2 reaction on Mo(110)−(1 × 6)−O, as determined by the formation of N_2 via atom combination at high temperatures (Table 2). Taken together, our data are all consistent with the initial dissociation of NO_2 to adsorbed NO and Mo═O on Mo(110)−(1 × 6)−O.

At higher NO_2 doses, the amount of N_2 formed is lower, which is again consistent with the inhibition of total reduction by the deposition of oxygen during reaction at low temperatures. More Mo═O is deposited at low temperatures for high NO_2 exposures, and thus, N_2 formation is inhibited. The lower yield of N_2 relative to NO for NO_2 reaction on the thin film oxide compared to reaction of NO on the same surface is also consistent with the inhibition of NO reduction by oxygen, particularly terminal oxygen. Again, low-temperature dissociation yields Mo═O and NO on the surface. The deposition of Mo═O from NO_2 changes the reaction environment for the remaining NO so as to inhibit additional O loss.

Surprisingly, very little N_2O is formed from NO_2 reaction, whereas N_2O is a significant product (comparable to N_2) of NO reduction on oxidized Mo(110). It is known from previous work that N_2O is primarily formed from oxygen loss from a dinitrosyl.[23]

The differences in selectivity for NO_2 versus NO reaction are most likely due to modification of the environment in which NO species react. As shown by the low-energy electron diffraction data of NO_2 on the Mo(110)−(1 × 6)−O surface, the adsorption of NO_2 changes the oxygen overlayer such that the (1 × 6) pattern is replaced by a diffuse (1 × 1) pattern. This indicates that oxygen is displaced from its most stable high coordination sites and that the surface disorders. This change in the oxygen overlayer could very well affect the selectivity for reaction either by limiting the availability of sites for O that

must be lost during reduction or by modifying the local bonding of the species on the surface.

Discerning the mechanism for NO_2 reduction is difficult because of the complexity of NO_2 behavior on the surface that is illustrated by our infrared studies. There are multiple species present on the surface at all temperatures studied and, significantly, at temperatures for which reduction occurs. Furthermore, there are no substantial differences in the types or amounts of species formed on the thin film oxide versus the chemisorbed oxygen layer. On both surfaces, N_2O_4, NO_2, monomeric NO, and dinitrosyl species are detected in infrared studies.

The presence of coupled NO_2 entities in the form of N_2O_4 raises the possibility of reduction via these coupled species. However, the high yield of NO and the presence of dinitrosyl are strong evidence that NO_2 reduction largely proceeds via NO formation followed by further reduction. The small amount of N_2 formed below 200 K could easily be accounted for by NO reaction.

Conclusions

NO_2 is reduced, releasing oxygen and NO to O-modified Mo(110) surfaces. Several different species are identified on the surface using infrared spectroscopy: N_2O_4, NO_2, monomeric NO, and dinitrosyl. The major product of NO_2 reduction is NO, although some reduction to N_2 is also observed. Surprisingly, there is very little formation of N_2O from NO_2 reaction, even though it is a significant product of NO reduction. Our experiments suggest that the overall oxidation state and the distribution of oxygen on the surface are important factors in determining the reactivity and selectivity for NO_2 reduction.

Acknowledgment. We gratefully acknowledge the support of this work by the US Department of Energy, Basic Energy Sciences, Grant No. DE-FG02-84-ER13289.

References and Notes

(1) Cant, N. W.; Liu, I. O. Y. *Catal. Today* **2000**, *2131*, 1.
(2) Penetrante, B. M.; Brusasco, R. M.; Merritt, B. T.; Vogtlin, G. E. *Pure Appl. Chem.* **1999**, *71*, 1829.
(3) Ammann, M.; Kalberer, M.; Jost, D. T.; Tobler, L.; Rossler, E.; Piguet, D.; Gaggler, H. W.; Baltensperger, U. *Nature* **1998**, *395*, 157.
(4) Grassian, V. H. *Int. Rev. Phys. Chem.* **2001**, *20*, 467.
(5) Bartram, M. E.; Koel, B. E. *Surf. Sci.* **1989**, *213*, 137.
(6) Polzonetti, G.; Alnot, P.; Brundle, C. R. *Surf. Sci.* **1990**, *238*, 226.
(7) Outka, D. A.; Madix, R. J.; Fischer, G. B.; Dimaggio, C. *Surf. Sci.* **1987**, *179*, 1.
(8) Koel, B. E.; G, W. R.; Bartram, M. E. *Surf. Sci.* **1987**, *184*, 57.
(9) Wickham, D. T.; Banse, B. A.; Koel, B. E. *Surf. Sci.* **1991**, *243*, 83.
(10) Schwalke, U.; Parmeter, J. E.; Weinberg, W. H. *J. Chem. Phys.* **1986**, *84*, 4036.
(11) Jirask, T.; Dvorak, J.; Rodriguez, J. A. *Surf. Sci.* **1999**, *436*, L683.
(12) Fuggle, J. C.; Menzel, D. *Surf. Sci.* **1979**, *79*, 1.
(13) Jirask, T.; Kuhn, M.; Rodriguez, J. A. *Surf. Sci.* **2000**, *457*, 254.
(14) Liu, G.; Rodriguez, J. A.; Hrbek, J.; Dvorak, J.; Peden, C. H. F. *J. Phys. Chem. B* **2001**, *105*, 7762.
(15) Rodriguez, J. A.; Jirask, T.; Sambasivan, S.; Fischer, D.; Maiti, A. *J. Chem. Phys.* **2000**, *112*, 9929.
(16) Rodriguez, J.; Jirask, T.; Liu, G.; Krbek, J.; Dvorak, J.; Maiti, A. *J. Am. Chem. Soc.* **2001**, *123*, 9597.
(17) Busca, G.; Lorenzelli, V. *J. Catal.* **1981**, *72*, 303.
(18) Rodriguez, J. A.; Jirask, T.; Dvorak, J.; Sambasivan, S.; Fischer, D. *J. Phys. Chem. B* **2000**, *104*, 319.
(19) Liu, G.; Rodriguez, J. A.; Hrbek, J.; Dvorak, J.; Peden, C. H. F. *J. Phys. Chem. B* **2001**, *105*, 7762.
(20) Rodriguez, J. A.; Perez, M.; Jirask, T.; Gonzalez, L.; maiti, A.; Larese, J. Z. *J. Phys. Chem. B* **2001**, *105*, 5497.
(21) Xu, C.; Hassel, M.; Kuhlenbeck, H.; Freund, H. J. *Surf. Sci.* **1991**, *258*, 23.
(22) Weldon, M. K.; Friend, C. M. *Surf. Sci.* **1994**, *310*, 95.
(23) Queeney, K. T.; Friend, C. M. *ChemPhysChem* **2000**, *1*, 116.
(24) Chen, D. A.; Friend, C. M. *Surf. Sci.* **1997**, *371*, 131.
(25) Chan, A. S. Y.; Deiner, L. J.; Friend, C. M. *J. Phys. Chem. B* **2002**, *106*, 13318.
(26) Bartram, M. E.; Windham, R. G.; Koel, B. E. *Langmuir* **1988**, *4*, 240.
(27) Queeney, K. T.; Friend, C. M. *J. Phys. Chem. B* **1998**, *102*, 9251.
(28) Louis, R. V. S.; Crawford, J. B. *J. Chem. Phys.* **1965**, *42*, 857.
(29) Koch, T. G.; Horn, A. B.; Chesters, M. A.; McCoustra, M. R. S.; Sodeau, J. R. *J. Phys. Chem.* **1995**, *99*, 8362.
(30) Nakamoto, K. *Infrared and Raman Spectra of Inorganic and Coordination Compounds*, 5th ed.; John Wiley & Sons: New York, 1997; Part A.
(31) Wang, J.; Koel, B. E. *Surf. Sci.* **1999**, *436*, 15.
(32) Queeney, K. T.; Friend, C. M. *J. Chem. Phys.* **1997**, *107*, 6432.
(33) Nart, F. C.; Kelling, S.; Friend, C. M. *J. Phys. Chem. B* **2000**, *104*, 3212.
(34) Fateley, W. G.; Bent, H. A.; B. Crawford, J. *J. Chem. Phys.* **1959**, *31*, 204.
(35) Queeney, K. T.; Friend, C. M. *Surf. Sci.* **1998**, *414*, L957.
(36) Wahlstrom, E.; Vestergaard, E. K.; Schaub, R.; Ronnau, A.; Vestergaard, M.; Laegsgaard, E.; Stensgaard, I.; Besenbacher, F. *Science* **2004**, *303*, 511.